Modeling and Experimental Results of Concentration with Support Material in Rapid Freeze Prototyping

Frances D. Bryant and Ming C. Leu
Department of Mechanical and Aerospace Engineering
Missouri University of Science and Technology
Rolla, MO 65409
fbryant@mst.edu, mleu@mst.edu

Reviewed, accepted September 10, 2008

ABSTRACT

Ice structures with complex geometries and overhung areas are created by the Rapid Freeze Prototyping (RFP) process in a sufficiently cool environment by freezing water into ice as the main material in conjunction with a eutectic dextrose-water solution as the sacrificial support material. The supported areas in an ice structure are removed via an increase in temperature in a separate environment after the structure is completely fabricated. To understand to what extent these two materials mix during fabrication, two methods of modeling the concentration changes that occur near the interface of the main and support materials have been developed. The simulation results based on these models along with some experimentally measured data are presented in this paper.

1. INTRODUCTION

A sub-zero temperature environment is utilized in the Rapid Freeze Prototyping (RFP) process to create ice parts. A sacrificial support material, which is a eutectic sugar-water solution, has been identified for making ice parts of complex geometries and overhung areas [1]. The support material used in RFP is miscible with the main build material, which is water that freezes to ice, so there is a potential of diffusion between the two materials. Both materials, support and main, are deposited in a layer-by-layer manner with a drop-on-demand nozzle. A schematic of this RFP process is shown in Figure 1. Extensive research has been conducted for this process, where only the main build material is concerned. A thermal model has been completed for use in determining temperature changes during new layer depositions in thin walls [2]. The geometric feature and surface finish of completed ice parts has also been studied [3,4]. Information regarding the fabrication of complex ice parts, however, has not received extensive studies. The research here is a continuation of the authors' recent work [5]. In the current work, two concentration models have been developed to analyze the physical process of RFP with both main and support materials. The results from these two concentration models are compared with each other and also with the measured experimental data.

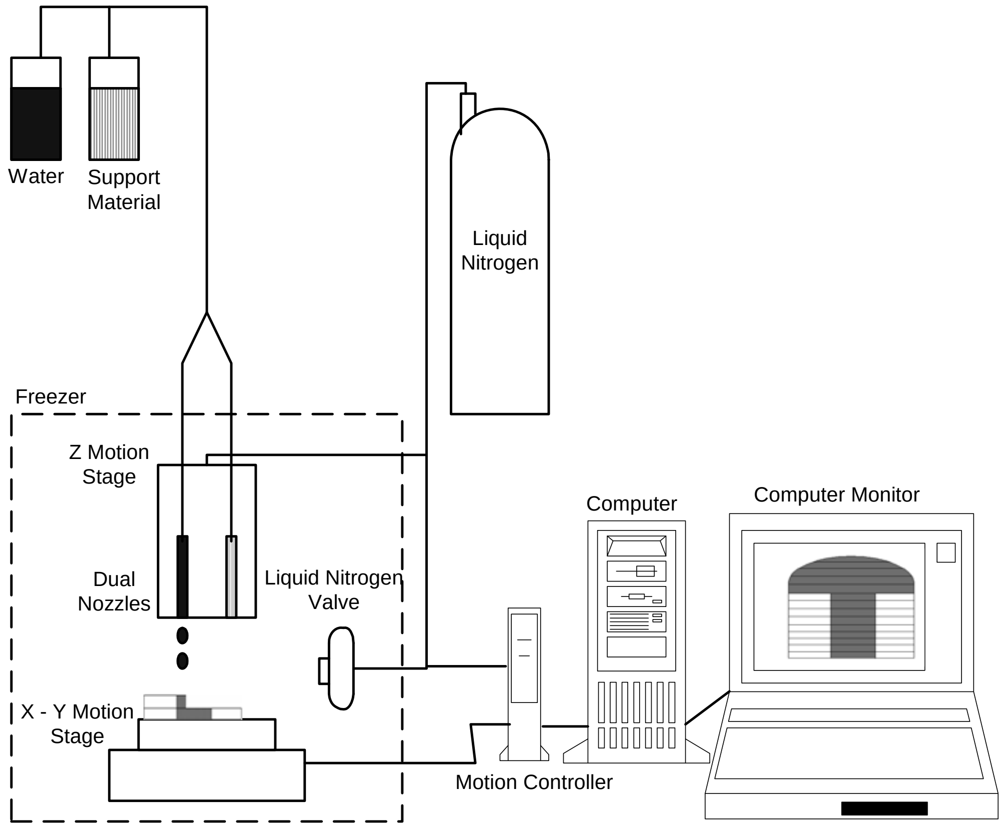

Figure 1: Rapid freeze prototyping schematic

Previous relevant work in various other part fabrication processes include laser surface alloying, selective laser sintering, and shape deposition manufacturing. Laser surface alloying, also known as laser cladding, is a process where a laser is used to heat multiple types of metal and/or metal powder in a controlled manner to alter physical properties or create a near net shape part. Kar and Mazumder's laser surface alloying model [6] assumed that solid-to-solid contact diffusion is not substantial. Selective Laser Sintering (SLS) is a process which uses a laser to fuse material in a layer-by-layer fashion and often utilizes two materials in the process. Chen et al. [7] published findings from a model using two metal powders in SLS regarding the temperature during the process and the dimensions of the heat affected zone (HAZ). A thermo-mechanical model was developed by Chin et al. [8,9] for the use in Shape Deposition Manufacturing (SDM). The thermo-mechanical model was developed using an uncoupled thermal and mechanical analysis. This model is general enough that the framework can be applied to some other SFF methods.

The research presented here is aimed at determining to what extent the design dimensions of an ice structure is compromised when the supported areas are removed for a completed part, and what build temperature is necessary to provide dimensional accuracy and prevent as much degradation to the ice part as possible. The presentation of the paper is as follows. Section 2 discusses the support material used in the process. Section 3 presents and discusses concentration modeling as well as compares the models presented to measured experimental data. Section 4 concludes the paper.

2. SUPPORT MATERIAL DISCUSSION

The sacrificial support material used in RFP is a eutectic dextrose/water ($C_6H_{12}O_6 - H_2O$) solution which is 33% anhydrous dextrose and 67% distilled water by weight. The solution was chosen due to the freezing point being slightly lower than that of pure water. The support material freezing point is -5.6 °C, which enables the supported areas to be removed between 0 °C and -5.6 °C once the ice part is completely fabricated. The support material is also an environmentally benign solution, so it is compatible with the green process intention of RFP. Figure 2 shows the phase diagram for the support material, noting the eutectic point is the most depressed point in the temperature-concentration curve. The properties for the support material which are used in the analysis presented in this paper are given in Table 1.

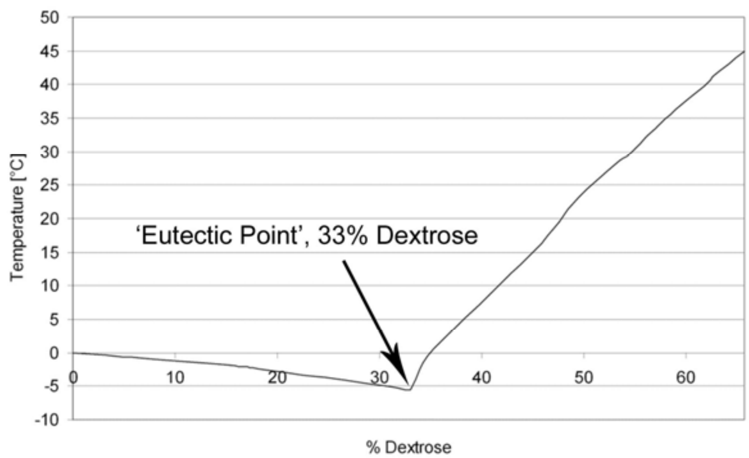

Figure 2: Phase diagram for a dextrose/water ($C_6H_{12}O_6 - H_2O$) solution

Since a constituent of support material is water, the main build areas (i.e. water/ice) and the areas of support material have a natural tendency to mix during fabrication. The dextrose in the supported areas will diffuse into areas of pure water, thereby reducing the concentration of dextrose in the supported areas and contaminating the main build feature areas. The mixing of the two materials is only considered significant when both materials are in contact and both are in liquid phase. The diffusivity of solid-to-solid contact, as well as solid-to-liquid contact is much lower than for liquid-to-liquid contact. Basically this means that very little dextrose will 'travel' into pure ice/water sections if the support material and main material areas are frozen [10]. The only time that both the support material regions and main build material regions are in liquid phase concurrently for a significant amount of time is when water is deposited onto an area of already frozen support material. This is because water has a higher latent heat than the support material, so as the water layer cools and freezes, the support material is prone to melting. If a like material (i.e. water on water or support material on support material) is deposited, there is not a potential for diffusion since the areas of concentration are the same in both locations. If the support material is deposited on already-frozen ice, the ice does not significantly melt since the phase change of the support material will not melt the existing ice section.

Table 1: Properties of water/ice and the sugar solution

	Water / Ice	Sugar Solution
Density: ρ_{solid} ρ_{liquid}	917 kg/m^3 1000 kg/m^3	917 kg/m^3 1140 kg/m^3
Specific Heat: c_{solid} c_{liquid}	2094 J/kg-°C 4174 J/kg-°C	1404 J/kg-°C 2800 J/kg-°C
Thermal diffusivity	1.146 X 10-6 m^2/s	1.146 X 10-6 m^2/s
Thermal conductivity	0.6 W/m-°C	≈ 0.6 W/m-°C
Latent heat of fusion	335000 J/kg	234000 J/kg
Heat transfer coefficient	8.66 W/m^2-°C	≈8.66 W/m^2-°C

When a frozen support section is being built upon by a new water layer, dextrose from the support material region of the wall will diffuse into the new layer of water due to the variation present in the concentration gradient. The diffusion process ends when the area is solidified due to freezing. A colder ambient temperature during fabrication will provide less time for diffusion to occur because of a shorter freezing time. A liquid nitrogen source is provided in the RFP setup in order to provide a very cold environment so that diffusion can be controlled by decreasing the freezing time. The cooling of the environment is somewhat a trade-off, however, since hardware has limitations of running in very low ambient temperatures. Liquid nitrogen can potentially decrease the ambient build environment to as low as -196 °C. Finding a balance of freezer temperature for faster ice part build time and lower diffusion between areas, yet warm enough for hardware requirements, has in part motivated this study.

The support material is not a pure substance. It is organic in nature due to the addition of dextrose, so the melting/freezing point is not an absolute defining line between liquid phase and solid phase. The support material goes through a ‘mushy’ zone between the phases. The support material removal process influences whether the ‘mushy’ zone will be removed or not. To remove the support material, a fabricated ice part was originally placed in an open ambient in a -5 °C freezer and left overnight to allow the supported regions to melt. This removal process left the interface of the main and support material very uneven. Figure 3 shows an interface where the support material has been removed and an uneven ice edge remains.

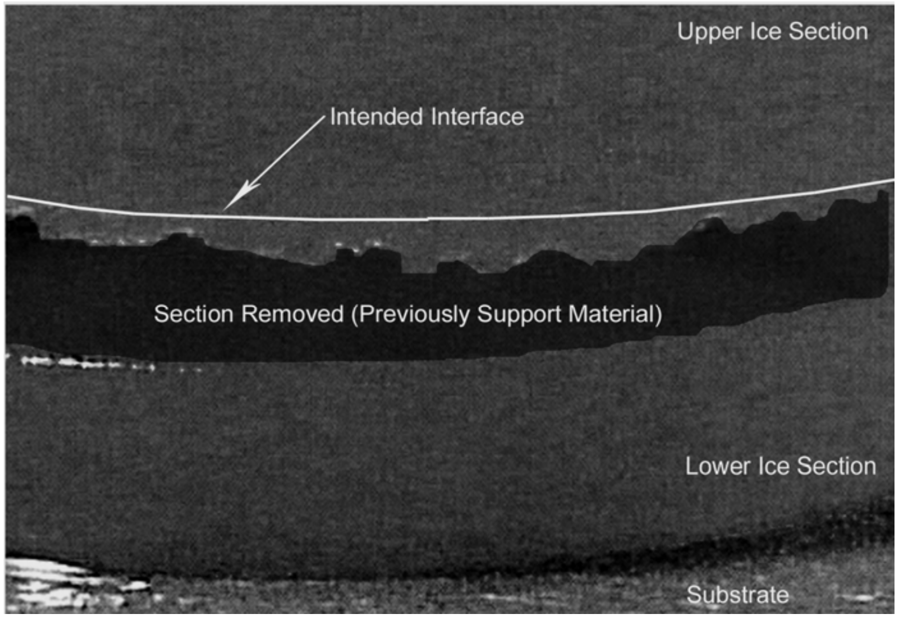

Figure 3: Uneven edge after support material removal in an open ambient

In order to remove the supported regions so that the interface is a smooth surface, the support material removal process evolved to placing the completed ice part in the -5 °C freezer in a kerosene bath and agitating the part until the supported areas were removed. By changing the support material removal process, the 'mushy' regions of support material are now removed from the part. The question arose as to how much dextrose must be present in the regions in order to remove that region during the support material removal process. To find out what concentration value in an area was being removed in the support material removal process, experiments were conducted. Lines of support material of varying thicknesses and dextrose concentration values, which represent different thicknesses of lines used in ice part fabrication, were deposited onto a substrate and allowed to sufficiently cool in a -25 °C ambient so the lines were completely frozen. The substrates were then transferred to a -5 °C freezer and the lines were put through the same process of support material removal as an ice part would be subjected to.

The results of the corresponding concentration values and thicknesses in which the lines were removed in the experiments are shown in Figure 4. The figure shows that as the thickness increases in a line, the percent of dextrose present in that area in order for it to be removed also increases. Thinner lines, and thus thinner ice structures, will be removed with less dextrose present in the areas during the support material removal. Depending on the thickness of ice parts being fabricated, Figure 4 can be referred to when determining at what concentration the supported areas will be removed. Typically, thin ice structures have a thickness of approximately 1- 2 mm.

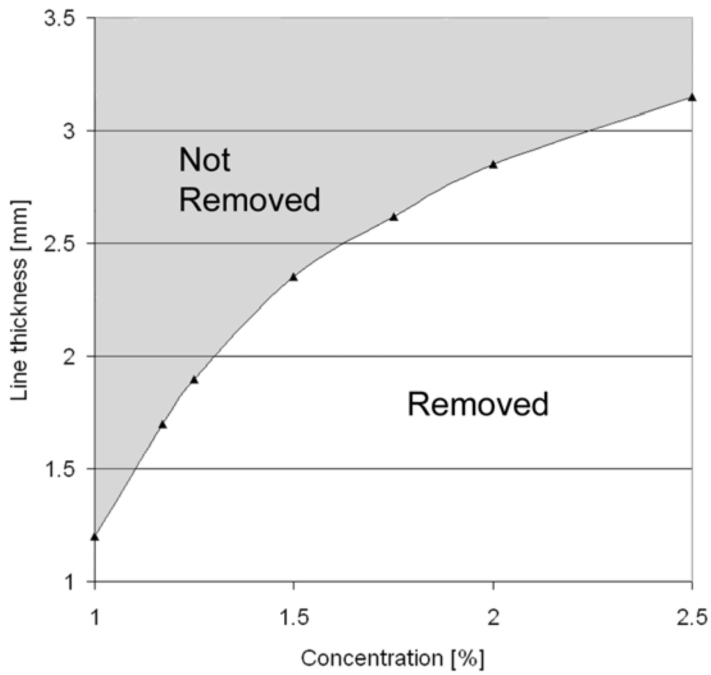

Figure 4: Concentration values for removal of support material at different line thicknesses

3. CONCENTRATION MODELING AND VALIDATION

The concentration model is closely tied to the temperature prediction model, which determines the temperature profile during fabrication. Diffusion occurs during liquid-to-liquid interaction of the main and support materials. The amount of time that each material is in liquid phase can be determined if the temperature is known for that material at any given time. The temperature model has been discussed in detail in a previous paper [5], but a synopsis is given here for clarification. The temperature in a thin wall is governed by the following equation [11]:

$$\frac{\partial T}{\partial t} = \frac{\lambda}{\rho c}\left(\frac{\partial^2 T}{\partial x^2} + \frac{\partial^2 T}{\partial y^2}\right) + q \qquad (1)$$

where T is temperature, t is time, x and y are spatial coordinates, q is the internal heat generation, λ is thermal conductivity, ρ is density, and c is specific heat. The modeling of a thin wall (i.e. two-dimensional wall) in RFP consists of two materials (main and support), a moving heat source and a phase change for both materials. The solution to this equation is approximated by implementing an FEA simulation due to the complex nature of the problem. Figure 5 shows the simulated temperature curves for two different ambient build temperatures. By knowing the ambient temperature during a build and using these simulated curves, a time length value can be obtained for when the new layer is in liquid phase.

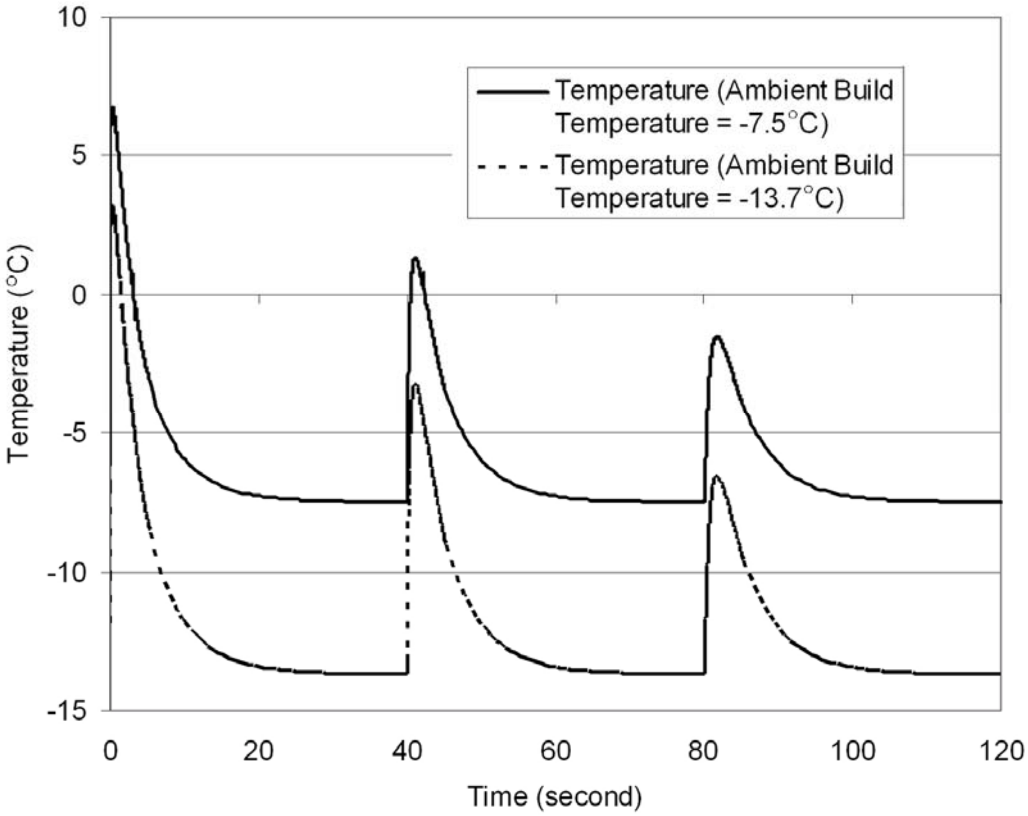

Figure 5: Simulated temperature during 3 layer depositions

To verify the temperature model, thin walls were built in the RFP freezer with a length of 20 mm and a height of 10 mm. Beaded wire, T-type thermocouples and a data acquisition board were used with a recording frequency of 5 scans per second to record temperatures at various locations. The ambient temperature was monitored to ensure a consistent (+/- 1° C) ambient build temperature during the entire fabrication time. The temperature at the transverse center of the wall at the interface of the two materials was monitored and recorded to compare with the temperature simulation. The water layer height was 0.2 mm, the wait time between layers was 40 seconds, the stand-off distance between the substrate and nozzle was 3 mm, and the build scan speed was 40 mm/s. The measurements and simulation results for an ambient temperature of -24 °C (a typical build temperature) is shown in Figure 6.

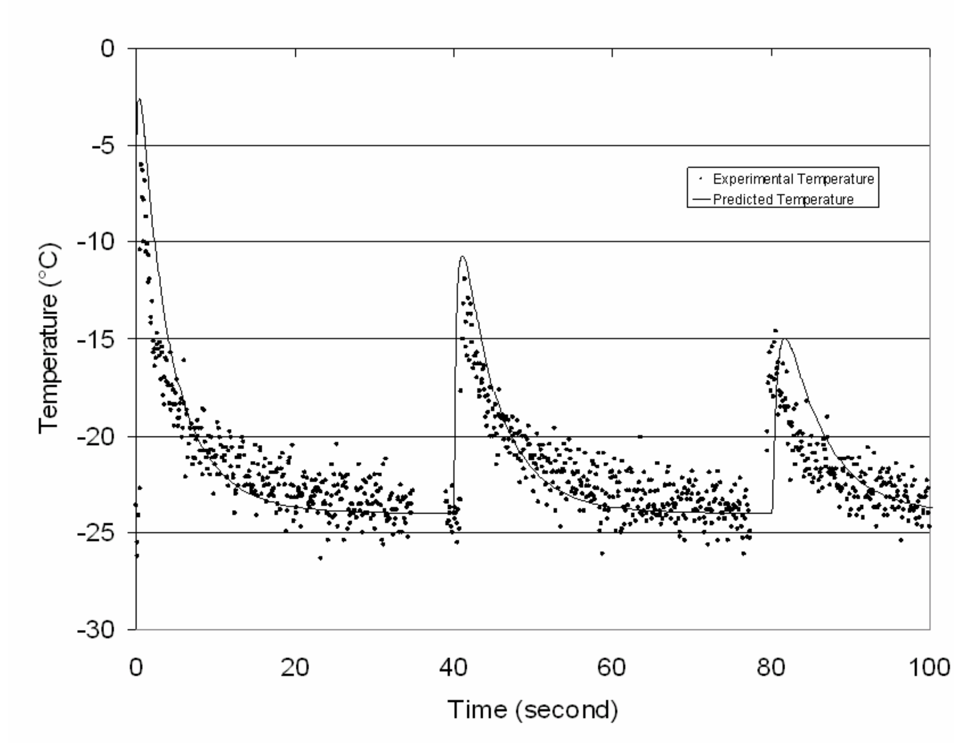

Figure 6: Temperature simulation results and experimental data for T_{amb} = -24 °C

Two methods of concentration prediction have been developed and will be outlined here. The model based on the first method is the continuous concentration model. This model is computationally efficient, but the model does not represent the physical process as accurately as the second concentration model, which is the discrete concentration model. The continuous concentration model takes into account a thin wall of support material with a thin wall of water/ice being deposited onto the already frozen wall of support material. The model simulates an 'infinite source' problem [12]. The entire support material area is available for dextrose to diffuse into the entire water area in this simulation. The time for the diffusion to occur is bounded by the time predicted in the temperature model where the interface temperature is above the melting temperature for both materials. This time is less for lower ambient temperatures since the materials freeze faster in a cooler environment. Figure 7 represents the continuous concentration model. The dextrose will distribute from the support material area into the water/ice area when the materials are in liquid phase, due to the concentration gradient present. Once the materials freeze, the diffusion is considered negligible.

The height 'a' shown in Figure 7 denotes the area of degradation in the ice structure where enough dextrose has migrated into the water region to cause it to be removed during the support material removal process. Determining dimension 'a' is the goal of the concentration model, since that dimension will represent how much of the intended ice structure is lost during the support material removal process due to diffusion.

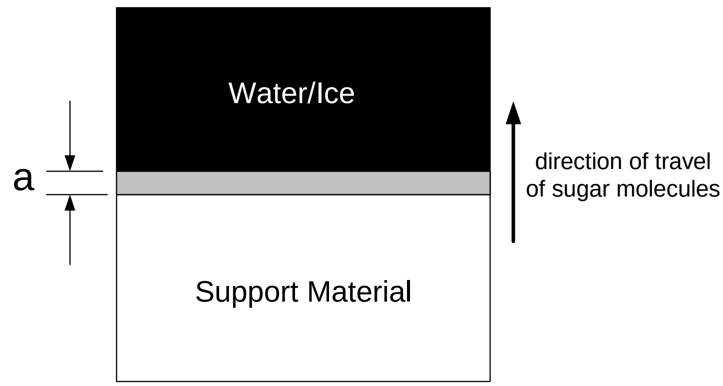

Figure 7: Continuous concentration model representation

The concentration in a thin wall as a function of time and location is governed by Fick's 2nd law, which for a two-dimensional case is the following equation [12]:

$$\frac{\partial C}{\partial t} = -D\left(\frac{\partial^2 C}{\partial x^2} + \frac{\partial^2 C}{\partial y^2}\right) \qquad (2)$$

where C is the concentration, D is the diffusion coefficient, t is time, and x and y are spatial coordinates. The moving source in the concentration model is negated because the results are changed only very slightly when a moving source is implemented, but computation time is drastically higher to implement a moving source [5]. The boundary conditions for this model are:

$$\begin{array}{llll} x = 0 & 0 \le y \le (h_1 + h_2) & t \ge 0 & \frac{\partial C}{\partial x} = 0 \\ x = L & 0 \le y \le (h_1 + h_2) & t \ge 0 & \frac{\partial C}{\partial x} = 0 \\ y = 0 & 0 \le x \le L & t \ge 0 & \frac{\partial C}{\partial y} = 0 \\ y = (h_1 + h_2) & 0 \le x \le L & t \ge 0 & \frac{\partial C}{\partial y} = 0 \end{array} \qquad (3)$$

The initial conditions are:

$$\begin{array}{llll} 0 \le x \le L & 0 \le y \le h_1 & t = 0 & C\ (x, y) = 33 \\ 0 \le x \le L & h_1 \le y \le h_2 & t = 0 & C\ (x, y) = 0 \end{array} \qquad (4)$$

Figure 8 shows a meshed FEA representation of the model. All the outer boundaries are considered to have a concentration flux of zero since diffusion can not occur across the boundary. The main and support materials are in contact at the interface once deposition of the water has occurred. If the temperature of the water (from the temperature model) is above the freezing temperature at any point after deposition, diffusion is assumed to occur until the time at which the water layer temperature goes below the freezing temperature of water.

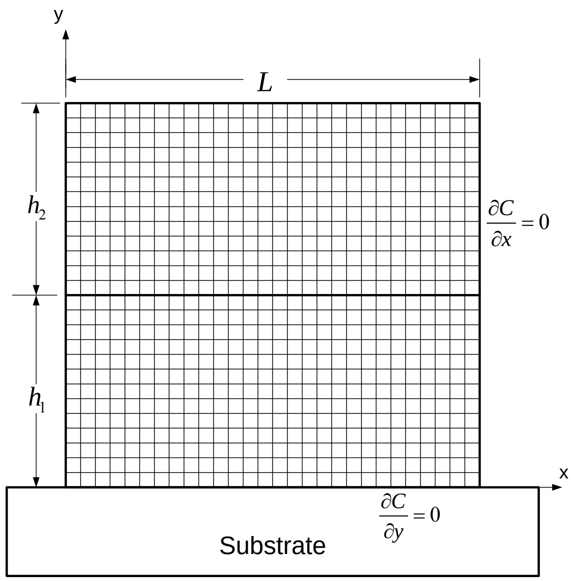

Figure 8: Continuous concentration model FEA representation

The simulation results of the continuous concentration model are shown in Figure 9. This figure represents concentration changes over time in the ice wall with respect to the y-axis direction. A removal concentration of 1% is shown in the figure with a dashed line. Using the amount of time the wall interface is in liquid phase from the temperature model, a final concentration value can be determined for varying depths into the ice portion of the wall. For instance, if the amount of time to consider diffusion is 10 seconds, the depth affected in the wall will be approximately 5 mm (i.e. where the 1% concentration line intersects with the depth/concentration line).

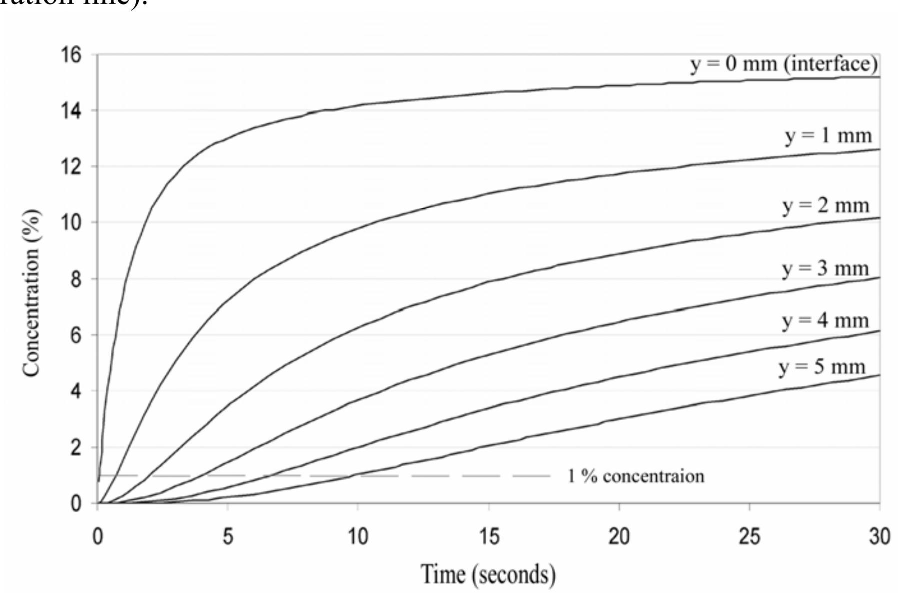

Figure 9: Predicted concentration at different heights in a thin wall

The second concentration model is the discrete concentration model. The computation time involved in this model is much higher than that of the continuous model. To compare, the discrete model took approximately two weeks to obtain results, due to the complex nature of a discretely implemented program. The continuous concentration model can generate results within 2-3 days, after the relevant data is obtained from the temperature model. Both models were run on a Dell Dimension desktop processor with a Pentium IV 3.2 GHz processor. The discrete concentration model considers a thin support material wall. The water layer deposition on top of the already frozen support material wall is implemented by discrete layer addition in this model. The initial conditions change for each new layer added. Changing the initial conditions each time a layer is deposited dramatically increases the complexity of the model. Figure 10 shows a representation of the discrete concentration model.

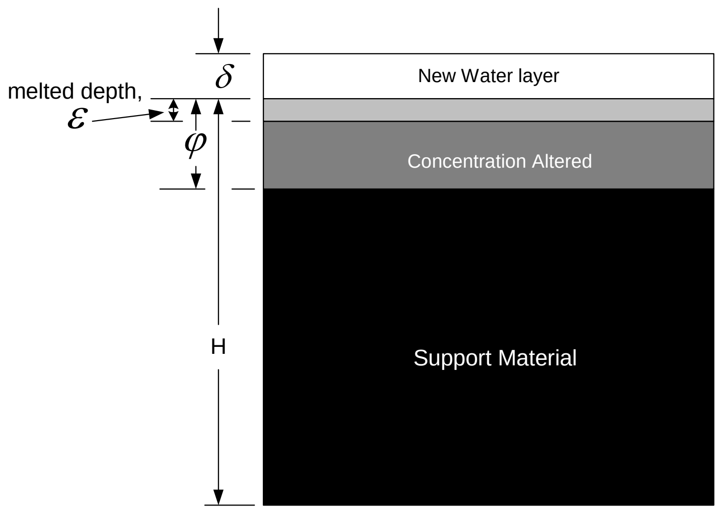

Figure 10: Discrete concentration model representation

For the first water layer deposited, φ will have a value of zero, but as layers are deposited, φ will change due to diffusion that occurs during the previous layer deposition. The melted depth, ε, is the depth to which the support material is available for diffusion. This depth is determined by using the temperature model and calculating to what depth, in the support material section of the wall, the temperature rises to above the freezing temperature of the support material. The melted depth is smaller for a lower ambient build temperature, due to the wall remaining colder and not being affected as much by the layer of warm water being applied.

The governing equation is the same as Equation 2 for the discrete concentration model. The boundary conditions are very similar to Equation 3; the only difference is that h_2 will only be one deposited layer in height, but representatively the boundary conditions still apply in the discrete model. The initial conditions, however, change and are computed each time a new layer is added from the previous layer-added simulation. The concentration in the wall isn't necessarily a constant value throughout the entire layer after diffusion has occurred. To represent the changing initial conditions, the concentration at the very top of each successive new water layer is shown in Figure 11 for varying build ambient temperatures. The concentration value shown for each new layer is after the wall is completely frozen and diffusion is ‘stopped’ until the next layer is added.

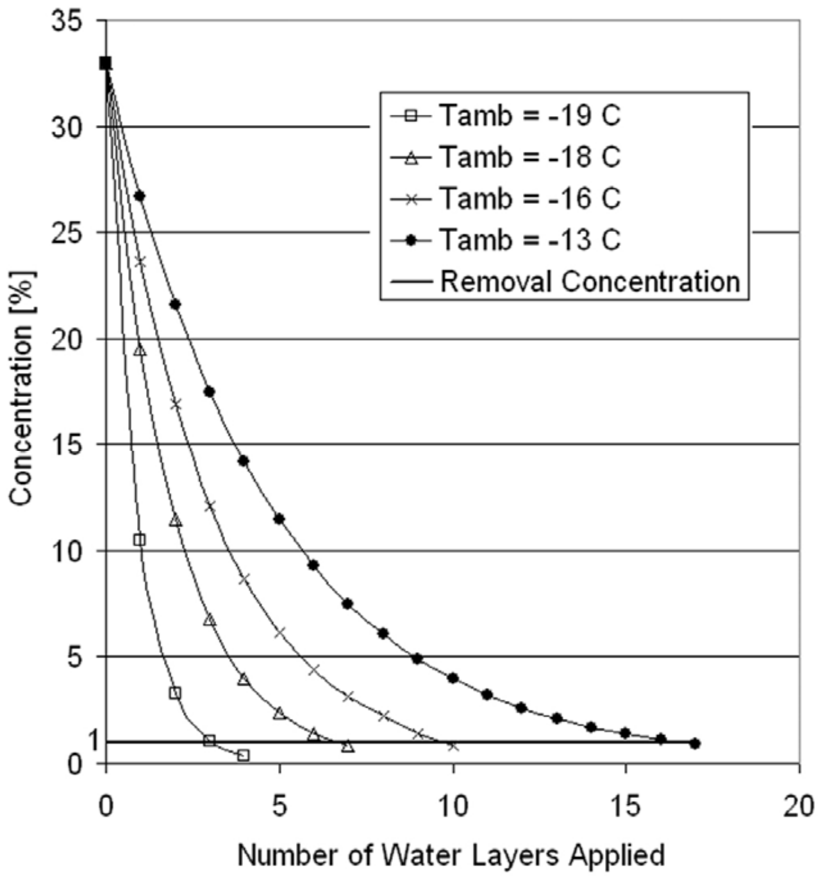

Figure 11: Top layer concentrations for varying ambient build temperatures

The first point for each curve is 33% because the history shown starts at the top of the support material wall, then the next point in each curve is the layer concentration at the top of the most previously deposited water layer, then the second deposited water layer, and so on. The model is run until the top layer concentration is < 1% dextrose. The 1% concentration value comes from Figure 3, which represents a concentration removal for a typical build wall thickness.

To show the discrete concentration model for a specific case, an ambient temperature of -19 °C is chosen. Figure 12 shows the concentration plots based on depths in a section of a thin wall. Frame 1 shows a lower layer of support material (i.e. 33%) and one layer of water (i.e. 0%) before any diffusion occurs. Frame 2 shows the second layer of water and it depicts the concentration changes that occurred before layer 1 was completely frozen. Frames 3-5 show the concentration changes for adding one additional layer for up to 5 layers of water. The dashed lines represent the melted depth, which is the depth that is melted due to the warm layer of water being applied. The labels ‘a – ee’ give a reference of location from frame to frame. The solid lines in the figure represent a complete layer, either of support material (the 33 % layer in Frame 1) or water. From Frame 5, it can be seen that two complete layers of water have concentration changes that are over 1 % dextrose and a partial layer (from d to dd) is also affected. The height above 'dd' has a low enough sugar content, that is considered 'not removed' and will remain a part of the completed ice structure.

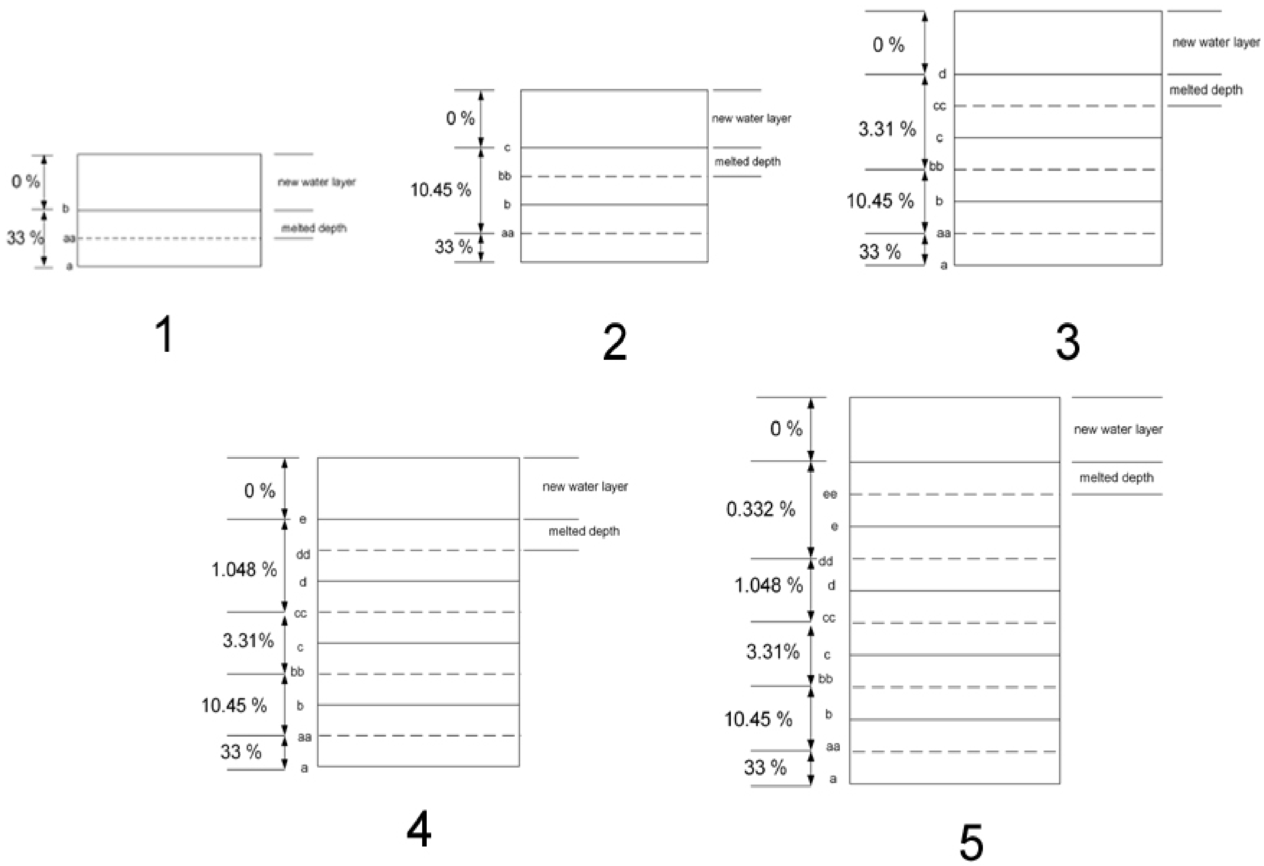

Figure 12: Concentration history for a wall built in -19 °C environment

In order to compare simulation results with experimental data, thin walls of support material on the bottom and ice/water on top were built in varying ambient temperatures. The walls had a length of 20 mm and a height of 10 mm each. The design dimensions for the test walls are shown in Figure 13. The fabricated walls were transferred to a kerosene bath at a temperature of -5 °C and agitated to remove the support material. Figure 14 shows an example of a fabricated test wall, as well as a close-up picture of an area affected by diffusion in a fabricated test wall.

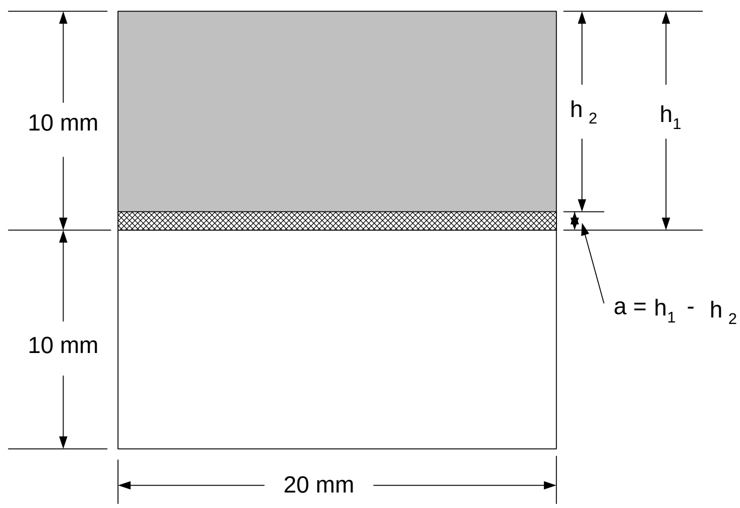

Figure 13: Experimental wall dimensions

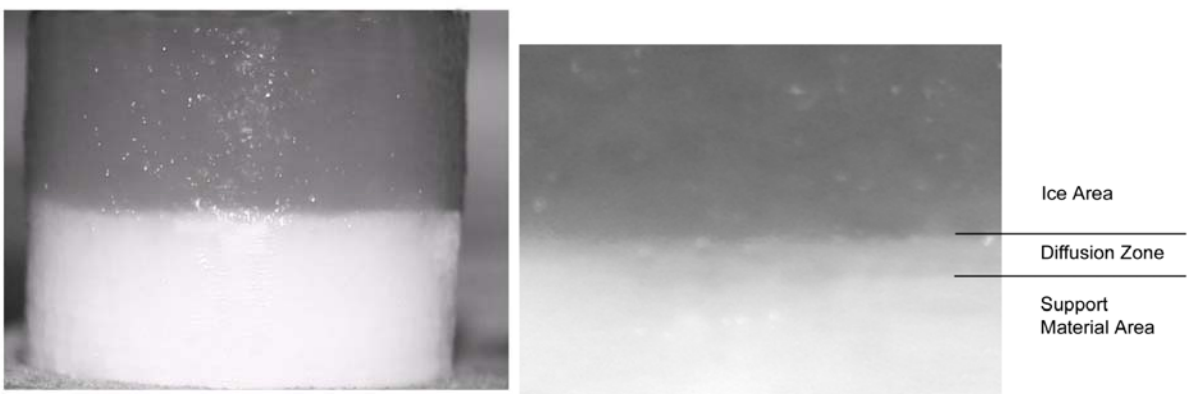

(a) (b)

Figure 14: Fabricated test walls with 2 different scenarios: (a) $h_1 = h_2$, (b) magnified view of a wall where $h_1 > h_2$

The concentration models were simulated to predict how much of the ice wall would be degraded due to diffusion of dextrose from the support material region to the water/ice region for varying ambient temperatures. Table 2 summarizes the results of the experimental data and the predicted wall height from each concentration model. The ambient temperature given is the environment temperature in which the walls were fabricated. The time that the new layer is in liquid phase and the melted depth of the layer which is being deposited onto is obtained from the temperature prediction model.

Table 2: Comparison of height data for ice parts built in varying ambient temperatures after support material removal, where T_{amb}=ambient build temperature, t_{liquid} = time predicted for materials to be in liquid phase, Melted depth = depth of melted support material, h_{pred} = predicted wall height for either model, $h_{measured}$ = average measured wall height after support material removal

T_{amb}	t_{liquid}	Melted depth, [mm]	Cont. Model h_{pred} [mm]	Disc. Model h_{pred} [mm]	$h_{measured}$	% Diff. Cont.	% Diff. Disc.
-13	1.3	1.5	8.45	8.30	7.79	5.68	3.97
-15	0.96	0.67	8.72	8.58	8.30	4.82	3.26
-16	0.81	0.51	8.80	8.71	8.65	1.70	0.69
-18	0.47	0.22	9.14	9.02	9.47	-3.6	-4.99
-19	0.22	0.10	9.60	9.50	9.67	-0.73	-1.79
-20	0	0	10	10	9.98	0.2	0.2
-21	0	0	10	10	10.05	-0.5	-0.5
-22	0	0	10	10	9.96	0.4	0.4

Figure 15 shows the height difference (intended build height minus height removed due to diffusion, or 'a' in Figure 13) between the measured experimental data and those predicted from the continuous concentration model and the discrete concentration model.

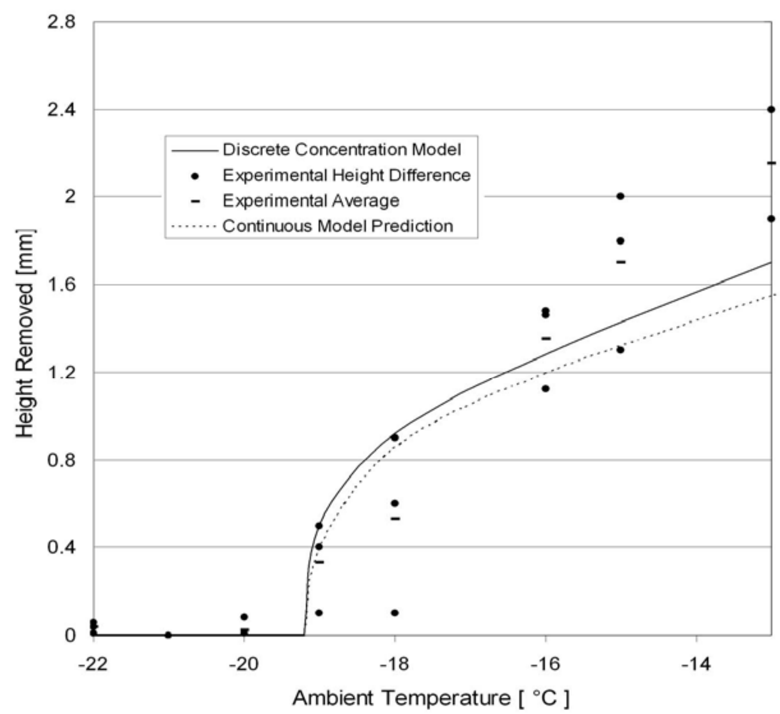

Figure 15: Discrete and continuous concentration model simulation results compared to experimental data

As an example of involving a support structure in ice part fabrication, Figure 16 shows a fabricated ice part with a supported center section. The left side of the figure shows the bridge-type part as fabricated with the support material still in the structure. The right side of the figure shows the part after the center supported region is removed.

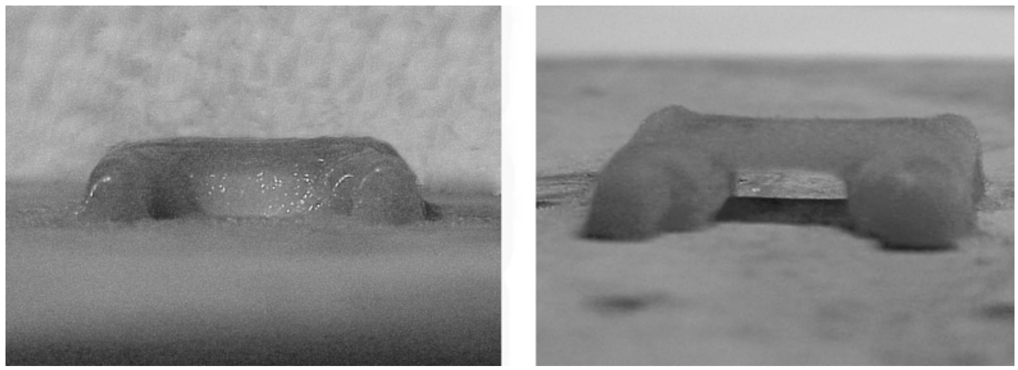

(a) (b)

Figure 16: A fabricated ice part with a supported center section: (a) before support material removal and (b) after support material removal

5. CONCLUSIONS

This paper has presented and discussed results of concentration models for the Rapid Freeze Prototyping process that uses a miscible support material during the part building process and removes the support material afterwards via a melting temperature difference. A two-dimensional thermal model simulating layer-by-layer processing provided information about temperature history, which was compared to experimental data obtained during an ice wall fabrication. Concentration models were presented, utilizing two modeling techniques to predict to what extent diffusion will alter final dimensions of thin ice walls. A removal concentration guideline was established to discern at what concentration value a diffused ice section will be removed in the support material removal process. Experiments were conducted to verify the two concentration models, and the experimental data was shown to have fairly good agreement with the simulation results obtained from either model.

ACKNOWLEDGMENTS:

The authors graciously acknowledge the financial support of the study from the National Science Foundation Grants DMI-0321712 and IIP-0637556.

REFERENCES:

[1] Bryant, F. and Leu, M. C., 2004, "Study on Incorporating Support Material in Rapid Freeze Prototyping", Proceedings of Solid Freeform Fabrication Symposium, University of Texas at Austin, Austin, TX.

[2] Sui, G. and Leu, M.C., 2003, "Thermal Analysis of Ice Wall Built by Rapid Freeze Prototyping", ASME Journal of Manufacturing Science and Engineering, Vol. 125, No. 4, November 2003, pp. 824-834.

[3] Leu, M. C., Liu, Q. and Bryant, F. D., 2003, "Study of Part Geometric Features and Support Materials in Rapid Freeze Prototyping", Annals of the CIRP, Vol. 52/1, pp. 185 – 188.

[4] Sui, G., Leu M., 2002, "Investigation of Layer Thickness and Surface Roughness in Rapid Freeze Prototyping", ASME Journal of Manufacturing Science and Engineering, Vol. 125, No. 3, pp 556-563.

[5] Bryant, F. and Leu, M.C., 2007, "Modeling and Validation of Temperature and Concentration for Rapid Freeze Prototyping", Proceedings of Solid Freeform Fabrication Symposium, University of Texas at Austin, Austin, TX.

[6] Kar, A. and Mazumder, J., 1988, "One-dimensional Finite-Medium Diffusion Model for Extended Solid Solution in Laser Cladding of Hf on Nickel", Acta Metallurgica, Vol. 36, pp. 701 – 712.

[7] Chen, T. and Zhang, Y., 2006, "Three-Dimensional Modeling of Selective Laser Sintering of Two-Component Metal Powder Layers", ASME Journal of Manufacturing Science and Engineering, Vol. 128, February 2006, pp. 299-306.

[8] Chin, R.K., Beuth, J.L. and Amon, C.H. 2001, "Successive Deposition of Metals in Solid Freeform Fabrication Processes, Part 1: Thermomechanical Models of Layers and Droplet Columns", Journal of Manufacturing Science and Engineering, Vol. 123, pp. 623 – 631.

[9] Chin, R.K., Beuth, J.L. and Amon, C.H. 2001, "Successive Deposition of Metals in Solid Freeform Fabrication Processes, Part 2: Thermomechanical Models of Adjacent Droplets", Journal of Manufacturing Science and Engineering, Vol. 123, pp. 632 – 638.

[10] Bird, R.B., Stewart, W.E., and Lightfoot, E.N., *Transport Phenomena,* 2nd Edition, John Wiley & Sons, Inc., Hoboken, NJ.

[11] Liu, Q. and Leu M.C., "Finite Element Analysis of Solidifying Processes in Rapid Freeze Prototyping", Proceedings of IMECE2004: ASME International Mechanical Engineering Congress, November 13-19, 2004, Anaheim, CA.

[12] Crank, J., 1956, *The Mathematics of Diffusion*, Oxford at the Clarendon Press, London.

[13] Bryant, F., Sui, G., and Leu, M. C., 2002, "A Study on the Effects of Process Parameters in Rapid Freeze Prototyping", Proceedings of Solid Freeform Fabrication Symposium, University of Texas at Austin, Austin, TX.

[14] Leu, M. C., Zhang, W., and Sui, G., 2000, "An Experimental and Analytical Study of Ice Part Fabrication with Rapid Freeze Prototyping", Annals of the CIRP, Vol. 49/1, pp. 147-150.

[15] Zhang, W., Leu, M. C., Ji, Z., and Yan Y., 1999, "Rapid Freezing Prototyping with Water," Materials and Design, Vol. 20, pp. 139-145.

[16] Chande, T. and Mazumder, J., 1983, "Composition Control in Laser Surface Alloying", Metallurgical Transactions B, Vol. 14B, pp. 181 – 190.

[17] Jackson, R.F., Silsbee, C. G., 1922, National Bureau of Standards Scientific Papers, Number 17, Vol. 17, No. 1404.

[18] Walas, S. M., 1985, *Phase Equilibria in Chemical Engineering*, Butterworth-Heinemann, Boston.

[19] Crank, J., 1984, *Free and Moving Boundary Problems*, Clarendon Press, Oxford.

[20] Rosenthal, D., 1946, "The Theory of Moving Sources of Heat and Its Application to Metal Treatments", Transactions of ASME, Vol. 68, pp. 849-866.